Smart Knife: Integrated Intelligence for Robotic Meat Cutting

A. Mason, D. Romanov, L. E. Cordova-Lopez, and O. Korostynska

***Abstract*—Automation is a key technology for a sustainable and secure meat sector in the future, both in terms of productivity and work environment. New robotic technologies, such as the so-called "meat factory cell," (MFC) aim to contribute to this goal, but they require new "smart" tools that provide sensor feedback, which enable robots to perform complex tasks. This article presents one such tool: the smart knife, which gives real-time feedback on its contact status with meat, as well as cutting depth. The tool and the system are described, and its operation evidenced via electromagnetic (EM) simulation using the Ansys High-Frequency Structure Simulator. Furthermore, the performance of the knife is validated using pork loin meat: in the worst case, knife is shown to have an error of 1.78% for contact detection, and a mean error of 7.66 mm (±1.45 mm) for depth detection. This article also presents brief discussion regarding eventual use of the knife as part of the MFC control system, in addition to future work to be performed.**

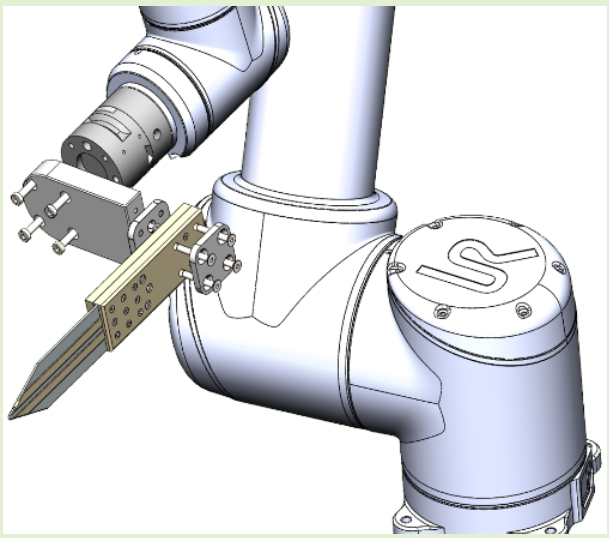

***Index Terms*—Microwave sensors, robot sensing systems, sensor systems and applications, smart knife.**

I. Introduction

WIDESPREAD availability of automation in the meat industry is a desirable goal for several reasons. Increased adoption of machines and robots is necessary to improve the sector's sustainability credentials, through increased production yield and efficiency. Furthermore, growing global demand for meat has increased pressure on the sector to raise production volumes. While automation has been available to the sector, its use is often limited for economic reasons: simply put, today's equipment is too expensive for the majority of small- and medium-scale processers and lacks reasonable financial (and technical) scalability. With increased customization for both hardware and software, robots can offer a flexible, scalable, compact, and cost-effective production line alternative to older machinery that require large floor space, are difficult to adapt, and include higher maintenance costs [1].

The sector is also often criticized due to the working conditions. That is, workers are typically performing repetitive tasks, often with a requirement for lifting heavy loads. Furthermore, those activities necessitate the use of dangerous equipment (e.g., knives and saws) and are often in environments suited to preserving product shelf life rather than human comfort. As a result, the sector suffers from high levels of absenteeism, injury, and early retirement [2], [3], [4]. During the Covid-19 pandemic, closure of meat processing facilities was commonplace, resulting in temporary reduction of productivity [5]. Largely, this can be attributed to high reliance on manual labor, in addition to tight working conditions. High dependency on humans, high demand for meat products, and high risks of injures on the factory floor—all these put the industry in a difficult position when it comes to recruitment. Experienced butchers often use, as they call it, the "just follow the knife" technique, that helps them to avoid muscle stress and further

Manuscript received 27 August 2022; accepted 15 September 2022. Date of publication 28 September 2022; date of current version 31 October 2022. This work was supported by the RoBUTCHER through the EU H2020 Program under Grant 871631. The associate editor coordinating the review of this article and approving it for publication was Dr. Kagan Topalli. *(Corresponding author: O. Korostynska.)*

A. Mason is with the Faculty of Science and Technology (REALTEK), Norwegian University of Life Sciences (NMBU), 1432 Ås, Norway, and also with the Norwegian Meat and Poultry Research Centre, Animalia AS, 0585 Oslo, Norway (e-mail: alex.mason@nmbu.no).

D. Romanov and L. E. Cordova-Lopez are with the Faculty of Science and Technology (REALTEK), Norwegian University of Life Sciences (NMBU), 1432 Ås, Norway (e-mail: dmytro.romanov@nmbu.no; luis.eduardo.cordova-lopez@nmbu.no).

O. Korostynska is with the Faculty of Science and Technology (REALTEK), Norwegian University of Life Sciences (NMBU), 1432 Ås, Norway, and also with the Department of Mechanical, Electronic and Chemical Engineering (MEK), Faculty of Technology, Art and Design (TKD), Oslo Metropolitan University (OsloMet), 0166 Oslo, Norway (e-mail: olga.korostynska@oslomet.no).

Digital Object Identifier 10.1109/JSEN.2022.3208667

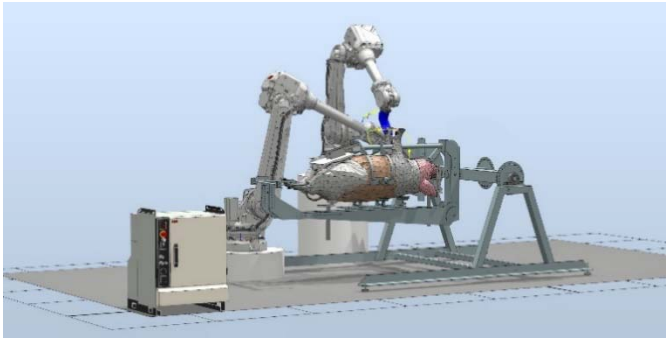

Fig. 1. MFC developed to provide access to automation particularly for small- and medium-scale meat processors.

development of related musculoskeletal disorders [6], but it takes time to gain this skill.

Automation is purported to benefit meat processing, both in relation to productivity and the working environment. This would alleviate supply-chain pressures during future pandemia and generally help processors maintain growth.

Alvseike *et al.* [7], along with key collaborators across Europe, have driven the development of a novel approach to meat processing in abattoirs, which is generally referred to the meat factory cell (MFC) [8]. This cell (see Fig. 1) implements an advanced robotic system to perform all the tasks of a traditional processing line, but within the confines of a robotic cell. These cells can be replicated, thus providing the economic and technical scalability that the sector misses today. Advanced robotic systems require harmonious co-operation between several subsystems, including robots (lifting and manipulation), artificial intelligence (scene recognition and path planning), tools (grasping and cutting), and sensors (real-time feedback and error detection). Meat processing tasks are challenging to automate, however, due to inherent variability; the MFC must adapt to process animals of different lengths, shapes, and weights, as well the heterogeneity of the raw material structure. It is, therefore, essential to have sensors and tools, which provide control feedback. Cutting is an important operation, as it directly affects yield and hygiene. The latter is particularly relevant, as the MFC uses an unconventional cutting regime [9], where the animal is dissected from the outside.

It is the importance of cutting within the MFC, or similar scenarios, that has been the motivation for this work. Smart cutting tools required, with the smart knife being able to analyze and predict the meat it cuts. Technologies with a potential of being used in a smart knife with possibilities of their integration into automatic meat processing were comprehensively reviewed in [10]. Optical methods, near infrared spectroscopy, electrical impedance spectroscopy, force sensing, and electromagnetic (EM) wave-based sensing approached were assessed against the set criteria. Optical methods are well established for meat quality and composition characterization [11], but lack speed and robustness for real-time use as part of a cutting tool. Methods, such as electrical impedance measurements [12] and rapid evaporative ionization mass spectrometry [13], are invasive and not suitable in meat processing, since they damage the meat. In meat industry, the application of the force sensing principle is based on the assumption that fat, meat, and cartilage will all require different forces to cut through, and measuring this force will, in turn, inform on the type of the tissue in contact with the knife, as was originally considered for surgical tasks [14]. However, slow response time and high cost of the built-in force sensors make it prohibitive option for automated meat cutting application. One attractive option is using athermal EM waves, as further explained in Section II-A.

The development of a smart knife capable of providing real-time feedback during robotic cutting in meat processing is reported. This article focuses particularly on the tool's capability to sense contact (i.e., with raw material) and depth. The smart knife was briefly reported earlier [15]; however, this article provides greater detail regarding the device design, its function, as well as deriving performance from a much larger validation dataset. Specifically, the sensing principle behind the smart knife, as well as detailed construction and design considerations are presented (see Section II-B), with physical, CAD, and high-frequency simulation software (HFSS) models shown. These are then compared with the results of the real manufactured prototype testing on up to 852 for each cutting depth, in steps of 5 mm in the 0–25-mm range.

II. Smart Knife

A. EM Sensing

The smart knife uses EM waves in the radio- and microwave range. The method detects changes in the EM field generated along a custom knife blade, which are caused by contact with materials. In this work, the main target material is pork meat. As the blade contacts and penetrates meat tissue, the permittivity to which the blade is exposed varies. The deeper the penetration, generally, the greater the average permittivity of the material immediately surrounding the blade. Those changes, through measurement of reflected S-parameter (S_{11}), are translated into information regarding the cutting status of the knife during robotic cutting. Specifically, information regarding contact (true of false) and cutting depth (in mm) is provided as the real-time feedback. These parameters are useful to determine correct operation, and further discussion on use of the smart knife is provided in Section IV-C.

The rational for incorporating sensing into a knife blade has been derived from experience. The MFC uses depth cameras to predict cutting actions; the existing depth cameras have an inherent error in depth estimation, which increases as a function of camera distance from a work object. Furthermore, at ≈400 mm, or less, from the work object, the camera cannot provide depth information at all. Added to this the risk of camera occlusion or contamination at close range to a work object, there is a clear need for on-tool intelligence.

Other methods for providing online feedback from a knife have been considered. Optical methods are well established for meat quality and composition characterization, but lack speed and robustness for real-time use as part of a cutting tool. Methods, such as electrical impedance measurements and rapid evaporative ionization mass spectrometry, are invasive and not suitable in meat processing, as they damage the meat. Based on a comprehensive review of methods for development of a smart knife [10], the use of a radio- and microwave-based smart knife is a novel approach. Nevertheless, the use

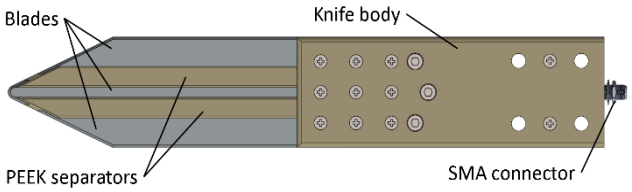

Fig. 2. CAD model of the knife showing the main external features.

of this technology has been slowly growing in the food sector, for example, in areas related to drip loss [16], freeze-thawing performance [17], and water activity [18], [19] measurement.

B. Construction and Design Considerations

The smart knife device (see Fig. 2) consists of three plates (Vanadis 4 Xtra steel, Uddeholm AB) separated by the polyether ether ketone (PEEK) dielectric material. The plates and the PEEK separators form the sensitive element of the smart knife. The two outer plates are electrically connected to the outer conductor of a coaxial cable (LMR240, Times Microwave Systems), while the central plate is connected to the core. Connection between the coaxial cable and the plates is enabled via a printed matching circuit in a coplanar configuration. The coaxial cable is directly soldered to the circuit board, while the plates have a mechanical fixing. The coaxial cable is terminated with a bulkhead SMA (female) connector, which is connected to a suitable measurement device [e.g., vector network analyzer (VNA)].

The body, or handle, of the smart knife is machined from PEEK. It houses the matching circuit as well as supporting the blade structure. The blades are secured in place by three stainless steel bolts per blade. Those bolts are isolated from the blades using dielectric spacers to minimize unwanted coupling or interference. The body also includes four mounting holes designed for adaptation of the smart knife to a robotic arm. The overall ideal length of the knife is ≈250 mm, while the blade is ≈125 mm (body to tip). The body is 45-mm wide. Those dimensions are correct according to the CAD model of the knife; the physical knife blade is a little shorter (≈122 mm) due excessive material removal during sharpening.

During the design of the knife, several factors have been considered, which are briefly described as follows.

1) Materials: The tool is constructed using of the Vanadis 4 Xtra steel, PEEK, and stainless steel. Vanadis 4 Xtra was chosen in consultation with an industrial steel supplier (Uddeholm AB, Sweden). This type of material is corrosion-resistant and tough. Stainless steel is commonplace in the food industry due to its corrosion resistance and robustness—the bolts, fixings, and exterior coaxial connector are all stainless steel. PEEK is less commonly used in the meat industry, however, and is considered food safe. It is a very durable material, having a high strength-to-weight ratio. In this application, it also an effective low-loss dielectric material [20], which is desirable for the proper operation of the sensing function.

2) Hygiene: The tool tolerates the use of hot water and alcohol-based agents used for disinfection. The isolators in the blade have a tight fit to the Vanadis plates, with 1-mm overlap to prevent fluids or biomaterial becoming trapped between the blades.

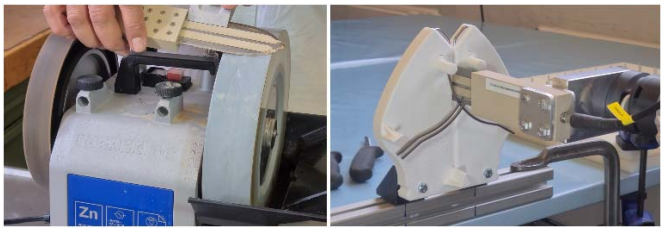

(a) (b)

Fig. 3. Sharpening of the smart knife using (a) grinding wheel (T-8, Tormek, Sweden) and (b) straightening tool (ERGO steel III, Bokken AS, Norway).

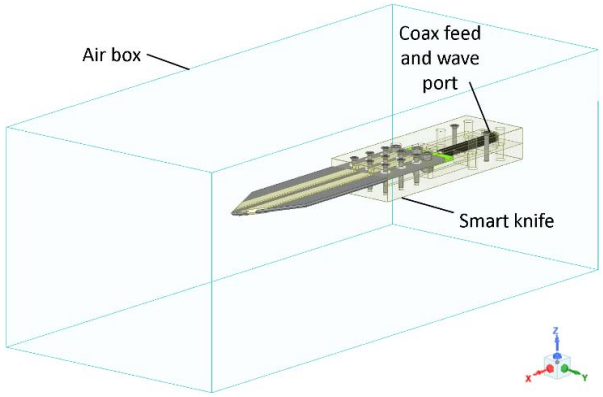

Fig. 4. HFSS model for simulation of the smart knife. The knife body has a high level of transparency to enable a view of the internal components.

3) Sharpening: The blade is sharpened by hand after assembly [see Fig. 3(a)] using a grinding wheel. It can be straightened more regularly between cuts using a device like that commonplace on today's meat processing lines [see Fig. 3(b)].

4) Robot Adaption: The double-edged blade reduces the need for 180° reorientation of the tool for multiple cuts along back-and-forth paths where only the height of cutting is varied.

5) Blade Length: Several iterations of blade length have been tested (physically). Shorter blades tend to make path execution and reorientation of the robot easier, whereas longer blades offer greater cutting depth per pass; 125 mm was a reasonable compromise between these competing factors.

C. Simulation

Simulation of the tool, both prior to construction, and for the purpose of refinement, has been useful to better understand its behavior. An assembly of the knife has been constructed in Solidworks (see Fig. 2) and can be imported into suitable software to allow full-wave EM field simulation. In this work, Ansys Electronics Desktop (2022) is used, namely, the HFSS module. An overview of the model is shown in Fig. 4.

The knife assembly, for simulation purposes, includes a coaxial connection, which extends from the internal circuit board to the rear outer boundary of the knife handle. In HFSS, the knife is surrounded by an air-box of 372.2 × 165 × 140 ($x \times y \times z$, in mm). The air-box boundary is configured to be radiant to model the knife in an open space, rather than a closed box. To prevent overlap of the air-box with the rear of the knife handle, a 1-mm extension of the coaxial cable is added in HFSS. A circular wave port excitation is added to the model, where the coaxial extension overlaps with the air-box boundary. The model is configured to have a solution

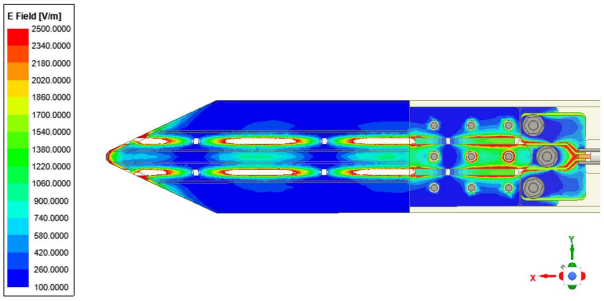

Fig. 5. Simulation of the EM field between the three plates comprising the blade. Several components of the model are set as fully or partially transparent to better illustrate the EM field.

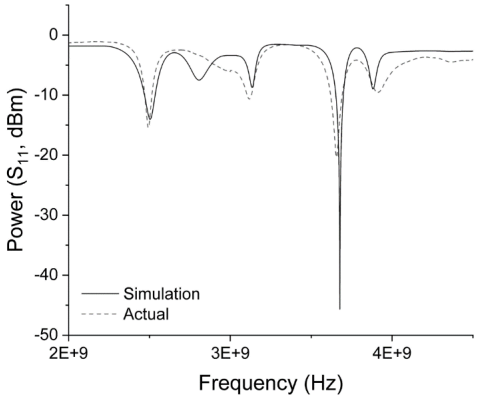

Fig. 6. Comparison of the simulated versus actual spectra in the 2–4-GHz region for the smart knife.

frequency of 4.5 GHz, with interpolating sweep between 2 and 4.5 GHz (4001 points). The conditions for convergence of the solution are as follows: 1) maximum passes (20); 2) minimum passes (6); and 3) minimum converged passes (3). All interpolating sweeps converged within 500 passes.

Simulation of the smart knife allows visualization of the EM field and its distribution along the plates comprising the blade, as shown in Fig. 5. The EM field travels between the plates toward the tip, and it is observed that the field also concentrates at the tip. This indicates that the knife will be most sensitive to interaction at or near the tip.

Simulation also gives an indication of resonant frequencies in the 2–4.5-GHz range. Accuracy of the simulation, compared with real-world performance, depends on several factors, including correctness (and availability) of material characteristics and production tolerances. In this case, most materials are available via the HFSS materials library, with the exception of the Vanadis 4 Xtra steel. In the absence of electrical characteristics from the manufacturer, it was replaced by a model for stainless steel. Furthermore, during production of a prototype, it was earlier noted that the physical length of the blade (from body to tip) is ≈122 mm, compared with the ideal length of 125 mm. Nevertheless, there is good agreement between the simulated and actual spectra for the knife, as illustrated in Fig. 6. Agreement between the simulated and actual performance provides a basis for demonstrating the expected response when the smart knife encounters raw material. From experience, the spectral regions around 2.5 and 3.65 GHz yield the most relevant information representing contact and depth sensing. Those are referred to as SR1 and SR2, respectively.

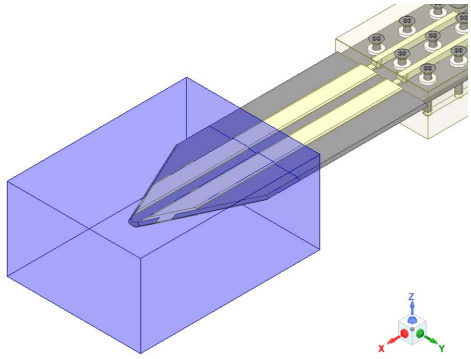

Fig. 7. Configuration of the HFSS model to include a water block, simulating the knife penetrating muscle tissue. Varying depths were simulated by varying the *x*-dimension of the block, between 0 and 60 mm, in 10-mm increments.

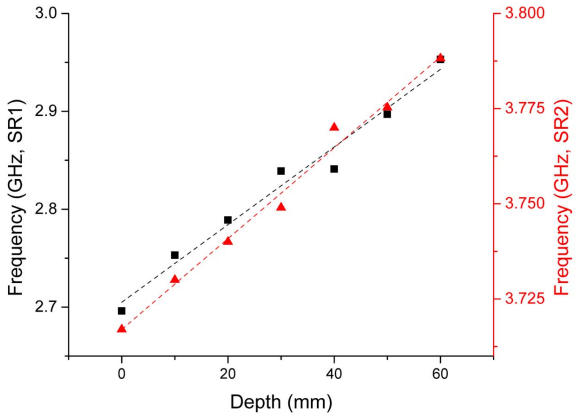

Fig. 8. Variation in resonant frequency for SR1 and SR2. Dotted lines show linear best fit for the respective region.

EM modeling of biological material directly is not trivial. Some proprietary human-body EM models exist, but their cost has been prohibitive for this work. A simpler approach has been applied in this work, using a water model to represent muscle tissue. This can be justified based on the relatively high-water content of fresh muscle tissue (≈75% [21]), which the smart knife would encounter in the MFC. A block of water was, therefore, added to the HFSS model, surrounding the blade (see Fig. 7). The block of water had the dimensions of 65 and 40 mm in y and z, and a variable length in x. An optometric analysis was performed, varying x between 0 and 60 mm, with 10-mm increments. At 0 mm, the extreme tip of the blade is not intersecting the water block—there is a small (<0.1-mm gap). Further iterations were not performed mainly due to the lengthy simulation time (approximately five days per iteration using a computer with 32-core processor and 96-GB memory).

Results comparing the shift in resonance are given in Fig. 8. The results track the frequency at which spectral minima occur in the 2.5- and 3.65-GHz regions. Correlation between frequency shift and depth can be described linearly for the two regions, where adjusted R^2 equals 0.972 and 0.986, respectively.

D. System Integration

The smart knife, as a system, consists of four main physical components (see Fig. 9). Those are briefly described as follows.

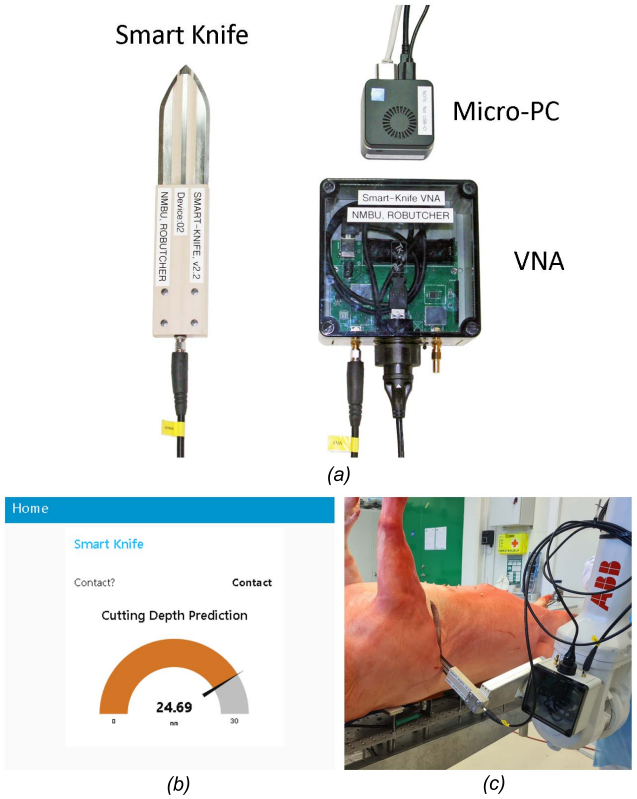

Fig. 9. Main components of the smart knife system. (a) Knife, VNA, and micro-PC and (b) Node-RED web interface running on the MCC, showing real-time contact and depth information. (c) Knife being used for trials in the MFC environment.

1) Knife: This interacts physically with the work object (e.g., meat and a carcass), enabling cutting as well as sensing of contact and depth.

2) VNA: A nanoVNA [22] device is used, with custom firmware (and IP65 housing) configured to disable unnecessary features and to optimize performance. The VNA connects to the knife via a coaxial cable.

3) Micro-PC: A 2.4-in device based on the Intel J4125 platform is used, running the Windows 10 Pro operating system. This runs custom software to control the data acquisition process from the VNA, to execute prediction models based on that data, via MATLAB, and to provide information of the knife status. The micro-PC also acts as a bridge between the VNA and the robot control, with possibilities for both wired and wireless Ethernet connection. The micro-PC is connected to the VNA via USB connection.

4) Main Control Computer: The MCC is the main control computer for the MFC and is common to all automation equipment within the cell environment. It implements generic control of the cell via workflows in Node-RED [23]. The MCC contains a specific node for the smart knife, which receives information from the micro-PC, exposing it to the workflow for corrective action and/or display for the user via a web user interface. The MCC receives data from the micro-PC via wired Ethernet connection.

III. Methodology

A. Equipment

The smart knife was fit to a UR10 (Universal Robots, Denmark), as illustrated in Fig. 10. The knife was also connected to a VNA, and that, in turn, to a micro-PC, as described in Section II-D. The MCC in the case of this work was a laptop computer, facilitating the collection of a data set for neural network model training, and knife performance validation.

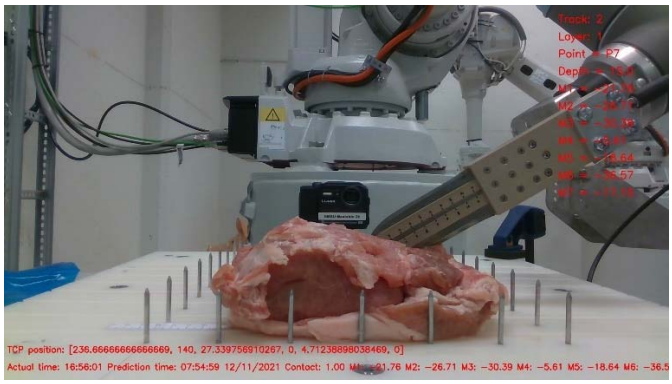

Fig. 10. Setup of knife and robot during meat cutting. The image is from an archive of each measurement point during validation and includes overlaid information regarding the cut at a specific point.

The knife was connected to port 1 of the VNA using a 2-m LMR240 coaxial cable with SMA-type terminations. The VNA was configured to sweep between 2.38 and 4 GHz, with a step size of 19.95 MHz (82 points). The nanoVNA can provide up to 201 points per spectra, but the elimination of redundant points provided some opportunity for optimization since previously reported work [8]. As the VNA has a sweep time of 2 ms per data point, the sampling rate of the smart knife was increased more than twofold. An open, short, and load calibration (ZV-135, Rohde & Schwarz, Germany) was performed on the coaxial cable, prior to attaching the knife. The calibration data are stored and loaded by the bespoke control software. Port 2 of the VNA was terminated with a 50-Ω load.

During validation, cuts of meat were placed on specially prepared nylon board with stainless steel spikes, which hold the meat in place. They are arranged in equally spaced tracks, with each having a 6-mm groove to allow the knife to completely cut through a sample without having to touch the board. The knife was configured to maintain an angle of 32.5° with the board, which had been established through trials and consultation with experienced butchers. The robot used a fixed movement speed of 50 mm/s, pausing for 1–2 s during data capture. A camera was positioned near to the cutting board, so that an image could be captured (see Fig. 10) along with every smart knife measurement. The image was overlaid with information, including a time stamp, tool position, and the outputs of various prediction models (see Section II-C). This was used for visual verification of the tool position during analysis.

The robot was controlled by a custom Python script running within the RoboDK simulation and programming environment. This also enabled capture of data from the smart knife, synchronized with image capture from the camera. A csv-format file provided output related to the position of the smart knife during each measurement and the outputs from various trained models (described in Section III-C). It also included the filename of the image associated with each measurement point.

B. Training Data Acquisition

Acquiring reliable training data in a controlled real-world setting is challenging for several reasons: variability in constitution, density, size, and shape, in addition to time-dependent factors, such as water loss. Fresh meat has a significant water content, however, to which the sensor technique applied here is highly sensitive. Therefore, a simpler, and more easily controlled, method for training the smart knife was devised, using only water. That procedure is as follows.

1) Fill a 30-L plastic container with ≈20 L of water.
2) Allow time for the water temperature to equalize with the surrounding environment (20 °C in this work).
3) Attach the knife to the UR10 robot and configure it, such that its center line (from the SMA bulkhead connector to blade tip) is oriented at 32.5° to the water surface.
4) With the knife positioned above the water, move it downward to the point where the knife is just touching the water surface. This is the zero point.
5) Move the knife to 100 mm directly above the zero point.
6) Initiate measurements, from +80 to −80 mm in 2-mm steps, where a negative value indicates the knife being in the water. Store data at each point for model training.
7) Repeat steps 4)–6), with the knife oriented at −32.5°.
8) Repeat steps 4)–6), with the knife oriented at 90°. In this case, the measurements in step 6) may be adjusted to be from +100 to −100 mm.
9) Repeat steps 4)–8) three times. It was found that this is not strictly necessary, as the correlation between the spectra was found to be high in this work ($R > 0.999$). However, in the case of some error occurrence during data capture, the added redundancy could assist in identifying data that should be discarded from training.

C. Model Generation

The data generated during the training data acquisition (described in Section II-B) was preprocessed into a unified csv-format file, where each spectra captured represented a single row in that file. The total number of spectra captured was 789, of which 390 represented no contact and 399 represented contact, with a depth of 0–100 mm. Two training sets were generated, one for contact, and one for depth.

Determining contact of the knife with the material is considered a binary problem: contact (1) and no contact (0). Therefore, data describing situations when the knife is either touching or below the water surface were defined as contact, and all other data described as no contact. For depth, the information required is a value representing the current cutting depth of the knife, in mm. The depth of the knife when it is not in contact with the meat was considered, at this stage, unimportant. The depth value was, therefore, classified as varying between 0 and −100 mm, with negative values indicating penetration. All data collected representing positive depth values (i.e., no contact) are classified as 0 mm.

Tools in MATLAB were used to produce prediction models for contact and depth. The specific tools used were contained within the MATLAB Deep Learning Toolbox: neural network pattern recognition tool (nprtool) for contact prediction and neural network fitting tool (nftool) for depth prediction.

TABLE I
CONFIGURATION PARAMETERS AND PERFORMANCE INDICATORS FOR MODELS GENERATED USING NPRTOOL AND NFTOOL

Model	Tool	Total data samples	Training, validation, testing samples	Network layers	Test CE/MSE[a]	Test %E/R[b]
Contact	nprtool	852	596, 128, 128	10	0.831	0.503
Depth_1	nftool	852	596, 128, 128	10	10.8	0.957
Depth_2	nftool	852	596, 128, 128	10	0.502	1.000
Depth_3	nftool	852	596, 128, 128	15	0.777	1.000
Depth_4	nftool	852	596, 128, 128	20	1.188	0.999
Depth_5	nftool	852	596, 128, 128	7	1.92	0.999
Depth_6[c]	nftool	486	340, 73, 73	10	3.05	0.998
Depth_7[d]	nftool	404	282, 61, 61	10	1.13	1.000

[a]nprtool indicates classification using Cross Entropy (CE); nftool provides an indication of the Mean Squared Error (MSE).
[b]nprtool indicates the percentage of samples which are misclassified (%E); nftool provides a correlation coefficient (R), indicating the fit, where a value of 1 is best.
[c]Only training data from 32.5° and -32.5° were included.
[d]Only training data from 90° were included.

A single model was generated for contact prediction using nftool, as the indicated error was found to be low, without the need for adjustment of default training parameters. However, depth prediction, with nprtool, proved a little more challenging. In total, seven models were produced for validation with meat, using several configurations, based on small pilot tests and subsequent iteration. Those configurations, and the resultant error or fitting indicators, are detailed in Table I. It is noted that the models Depth_1 and Depth_2 were generated using the same parameters; the difference in performance is indicative of the variable nature of such models.

The generated models were exported from MATLAB and bundled together into a standalone executable, which could receive input spectra and output prediction values for all models. This executable was incorporated into the custom software controlling the smart knife operation, so that the output values could be used for validation purposes when cutting meat.

D. Validation With Meat Samples

Pork loins ($n = 4$) with ≈2–4-mm surface fat, in addition to marbling within the muscle tissue, were used for the validation of the smart knife sensing capabilities. These were chosen to be broadly representative of the cutting anticipated to take place in the MFC. The meat was acquired fresh from slaughter and chilled for several days prior to the work taking place. The samples were allowed to equilibrate to room temperature before cutting, mainly since the overall of objective of the MFC is to work with hot (not chilled) carcasses.

Two cutting schemes were employed, one that performed a single cut of a specified depth per track, and the other that cut multiple times, with progressive depth, within each track. Those cutting schemes are referred to as single-depth and multidepth, respectively. The purpose of this was to consider how the knife performed in both situations, to aid with improving robustness for real-world implementation.

To configure each cutting scheme, the robot was first programed to follow a five-point path above the surface of the meat, representing the case of contact, but with a negligible cutting depth. The purpose of this procedure was to calibrate the height of the meat (i.e., to define a zero position at each

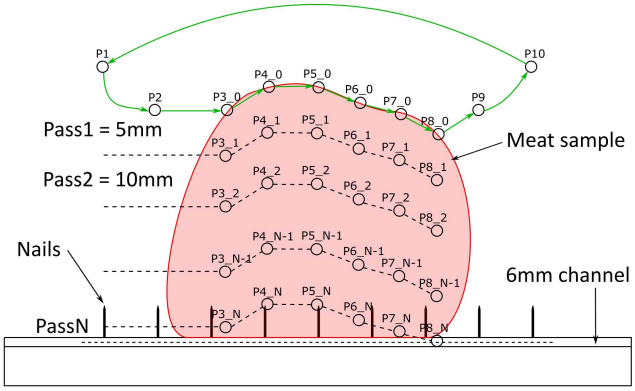

Fig. 11. Cutting path of the robot during the experimental work. Each pass of the robot consisted of ten points (P1–P10). The depth of cut, and if cutting was incremental, depended on the cutting scheme applied (i.e., single-depth or multidepth).

TABLE II
OVERVIEW OF DATA COLLECTED USING THE SINGLE-DEPTH AND MULTIDEPTH CUTTING SCHEMES

	Single-depth	Multi-depth
n, total	101	450
n, contact	55	254
n, no contact	46	196
n, depth = 0 mm	25	25
n, depth = 5 mm	6	26
n, depth =10 mm	6	26
n, depth =15 mm	6	28
n, depth = 20 mm	6	30
n, depth >= 25 mm	6	120

of the five points), so that adjustments could be made to the assumed knife depth during subsequent cutting.

The robot would then perform a cut including the aforementioned five-point path, where the position of each point was calculated programmatically using the zero position, plus a height offset. In addition, five further points were included in the path to make a cyclic motion for cutting, or a complete pass (see Fig. 11). Data were also collected at those points, which can be considered as no contact and zero cutting depth. Typically, each set of ten points included five contact and five no contact cases, with a deviation of ±1 contact point, caused by some irregularity in the shape, size, and surface of the loins. In total, 101 and 450 data points were collected for the single-depth and multidepth cutting schemes, respectively (see Table II for further details).

For the single-depth cutting scheme, offsets of 5, 10, 15, 20, and 25 mm were used. For each depth, measurements with a zero offset were also recorded. Each offset was applied once and required two loins. For the multidepth scheme, offsets in the range 0–40 mm were applied, in 5-mm steps. Four complete multidepth cuts were made, requiring a further two loins.

IV. RESULTS AND DISCUSSION

A. Contact Detection

Contact detection was determined using a single model, as noted in Table I. The model is a binary classifier, therefore outputting a value between 0 (no contact) and 1 (contact). In most cases, the output value is close to those extremities, but some exceptions were noted during initial testing. A threshold was, therefore, applied, where the values ≥ 0.3 imply contact.

With the single-depth cutting scheme, 55 of 101 data points had a verified contact condition; this was observed by the knife with zero error. For the multidepth cutting scheme, 254 of 450 data points had a verified contact condition. In this case, eight data points (1.78%) exhibited an error. The cause of the error has been unclear, but in at least half of the cases, a software error is suspected; either failed synchronization between the robot and the smart knife, or failure of the VNA software. However, at least one error was observed due to a large piece of muscle or fatty tissue clinging to the knife blade after completing a pass. The error cleared on the next pass due to contact with the loin, which removed the contaminant.

It was also observed with the multidepth case that there is a cumulative drift of the model output. As the number of cutting actions increases, the model output increases from 0, but never exceeded the threshold value during testing. Based on the inspection of the image data captured, it is suspected that this is caused by buildup of a film along the knife surface over time. Model output values greater than 0 started to be observed after ten passes of the knife and could indicate when cleaning is required. The knife, in this work, was cleaned only between tracks with an alcohol wipe; no specific method for cleaning has yet been established.

TABLE III
STATISTICAL INFORMATION DERIVED FROM SINGLE-DEPTH AND MULTIDEPTH CUTTING SCHEMES IN RESPECT OF DEPTH SENSING: MEAN ERROR (IN mm), AND 95 CONFIDENCE INTERVAL (95% CONF., IN mm)

	Depth model (Depth_*x*, as per Table 1)						
	1	2	3	4	5	6	7
Single depth:							
Mean error	12.28	4.98	5.92	9.06	7.78	5.56	6.13
95% conf.	4.03	1.99	2.08	2.74	3.75	2.00	2.11
Multi-depth:							
Mean error	11.46	7.66	8.03	8.97	8.78	7.91	10.37
95% conf.	2.23	1.45	1.32	1.29	1.46	1.10	1.48

B. Depth Detection

Results for all models are presented in Table III. From the seven models presented in Table I, it was Depth_2, which provided the best outcome in both the single-depth and multi-depth cutting schemes. An error of 4.98 mm (±1.99 mm) was observed for the former scheme and 7.66 mm (±1.45 mm) in the latter. It is noted that Depth_6 also yields comparable results, with a smaller confidence interval (±1.45 mm) in the later scheme but larger mean error (7.91 mm).

With both Depth_2 and Depth_6 models, it is obvious that error increased in the multidepth versus single-depth case. It is possible that this is due to the larger dataset from which statistical information is drawn. However, it could also be due to some uncertainty related to accumulated error in the actual robot position during this trial. The robot used has a reported position repeatability of ±0.1 mm, but when used for tasks, such as cutting, which require the robot to exert force on the work object, the authors have observed the robot tool center point to be some distance from its expected position, with respect to the board. For a single pass, the deviation observed in the offset height from the top of the loin was typically in the

range of 0.5–0.9 mm, but for several passes (as in the case for the multidepth cutting scheme), it could accumulate to several mm. For example, when the target depth was 40 mm, the robot reported an actual height offset between 40.7 and 46.9 mm.

C. Using the Smart Knife

The results presented confirm that the smart knife can determine contact and depth with a reasonably small error. As noted in Section I, the purpose of this knife is to provide a greater level of intelligence to the robotic cutting process within the MFC. It also helps to overcome some limitations observed when using depth cameras for predicting robot paths. It is necessary, however, to consider ways to incorporate the knife not only as a sensor (providing feedback), but also as a source of control within the robotic cutting process (enabling intervention or adaptation). This, of course, assumes that the knife can provide regular feedback regarding contact and depth status. Such consideration is an on-going process, but there are several scenarios under consideration. They include the following.

1) Verification of "Ready to Start Cutting" State: When a cutting operation is requested, the robot responsible must move to a starting position. Contact status from the knife (i.e., positive contact is detected when moving to a start position) will provide certainty of a valid starting position being attained, enabling cutting to commence, or giving the opportunity to adjust the starting position until contact is detected.

2) Verification of "Cutting Completed" State: It is difficult for a vision system to maintain a good view of a work object throughout a cutting process. This is due to the risk of contaminating the camera lens, as well as there being numerous ways that the view can be obscured (other equipment, the work object, and so on). Therefore, when there is a change from a positive to negative contact state during cutting, a means to terminate the cutting process is provided.

3) In-Process Path Adjustment: Cutting paths executed by a robot in the MFC are determined in advance of a cut taking place using a 3-D vision system. However, during processing, the biological material can and will change shape or otherwise deform. This can lead to variation in cutting depth along preplanned paths; the smart knife gives scope to adjust and maintain a consistent cutting depth.

4) Identification of an Error State During Cutting: There are several possibilities for error during a cut, including early completion (i.e., no contact but predicted cutting movement remains in-progress) and incomplete cutting (i.e., path complete, but knife still detecting tissue contact). Earlier than expected contact during cut startup or completion could also indicate unintended collision of the knife with some part of the work object. Furthermore, for certain cuts, the knife being too deep could also generate an error state. For example, in the MFC, there are cutting tasks around the rear limbs of a pig carcass close to the rectum and abdominal wall; cutting too deep in those areas could present a hygiene risk.

V. Conclusion and Future Work

Meat processing is an industry that requires novel automated solutions to remain sustainable and to mitigate harsh working conditions, shortage of skilled labor and not least, minimize impact of recent pandemic, which caused closure of many meat factories for hygiene and infection prevention reasons. Automation of all or many processes is seen as a way forward, but cutting meat requires novel smart tools. This article presents a novel smart knife tool, which uses an EM wave sensing technique to determine the status of the knife, namely, whether it is in contact with a work object, and its cutting depth. Simulation shows the basic principle of operation, such that the resonant frequency of the device shifts, as the surrounding permittivity changes; this makes it ideal for work with fresh meat where there is a high concentration of water. Experimental work to validate the performance of the device has been presented, where the device has been used to cut several loins using two different cutting schemes. In the worst case, the device was able to determine contact with an error of 1.78% and depth with a mean error of 7.66 mm ($\pm$1.45 mm). It is noted that further work with the device software may improve the reported contact error.

The work to date presents the first working prototype of the smart knife tool, which is the subject of a patent application [24]. There are, however, several areas where work continues to improve the tool to ensure its applicability to be used in robotic cutting. These include the following: 1) implementation of methods for rapid and frequent cleaning of the knife blade; 2) higher accuracy training models; 3) hygienic design considerations; 4) adjustments in the design to ease assembly; and 5) broadening of the sensor capability. Regarding the last point, of particular interest are establishing a means to verify if it is possible for the knife to sense proximity (rather than only physical contact), as well as to distinguish variation in material properties. These properties will enrich the feedback possibilities, allowing the robotic system to respond to events prior to cutting, as well as adjusting paths to avoid materials, such as bone.

Acknowledgment

The authors would like to thank the input of Øyvind Hansen and colleagues at the Norwegian University of Life Sciences (NMBU), Ås, Norway, for assistance in manufacture of the smart knife tool. They would also like to thank RoBUTCHER Consortium for their assistance in guiding the knife design, particularly Per Håkon Bjørnstad and Torunn Thauland Håseth at Animalia AS, Oslo, Norway, and Oddgeir Auklend at Robot Norge AS, Klepp Stasjon, Norway.

References

[1] D. Romanov, O. Korostynska, O. I. Lekang, and A. Mason, "Towards human-robot collaboration in meat processing: Challenges and possibilities," *J. Food Eng.*, vol. 331, Oct. 2022, Art. no. 111117, doi: 10.1016/j.jfoodeng.2022.111117.

[2] B. J. van Holland, R. Soer, M. R. de Boer, M. F. Reneman, and S. Brouwer, "Workers' health surveillance in the meat processing industry: Work and health indicators associated with work ability," *J. Occupat. Rehabil.*, vol. 25, no. 3, pp. 618–626, Sep. 2015, doi: 10.1007/s10926-015-9569-2.

[3] R. L. Dalla, A. Ellis, and S. C. Cramer, "Immigration and rural America," *Community, Work Family*, vol. 8, no. 2, pp. 163–185, May 2005, doi: 10.1080/13668800500049639.

[4] M. Broadway, "Meatpacking and the transformation of rural communities: A comparison of Brooks, Alberta and Garden city, Kansas," *Rural Sociol.*, vol. 72, no. 4, pp. 560–582, Dec. 2007, doi: 10.1526/003601107782638701.

[5] J. E. Hobbs, "The COVID-19 pandemic and meat supply chains," *Meat Sci.*, vol. 181, Nov. 2021, Art. no. 108459, doi: 10.1016/j.meatsci.2021.108459.

[6] N. F. Dias, A. S. Tirloni, D. C. D. Reis, and A. R. P. Moro, "Risk of slaughterhouse workers developing work-related musculoskeletal disorders in different organizational working conditions," *Int. J. Ind. Ergonom.*, vol. 76, Mar. 2020, Art. no. 102929, doi: 10.1016/j.ergon.2020.102929.

[7] O. Alvseike, M. Prieto, K. Torkveen, C. Ruud, and T. Nesbakken, "Meat inspection and hygiene in a meat factory cell—An alternative concept," *Food Control*, vol. 90, pp. 32–39, Aug. 2018, doi: 10.1016/j.foodcont.2018.02.014.

[8] *RoBUTCHER—A Robust, Flexible and Scalable Cognitive Robotics Platform*. Accessed: 2022. [Online]. Available: https://robutcher.eu

[9] O. Alvseike, M. Prieto, P. H. Bjørnstad, and A. Mason, "Intact gastrointestinal tract removal from pig carcasses in a novel meat factory cell approach," *Acta Veterinaria Scandinavica*, vol. 62, no. 1, p. 47, Dec. 2020, doi: 10.1186/s13028-020-00546-y.

[10] A. Mason, D. Romanov, L. E. Cordova-Lopez, S. Ross, and O. Korostynska, "Smart knife: Technological advances towards smart cutting tools in meat industry automation," *Sensor Rev.*, vol. 42, no. 1, pp. 155–163, Jan. 2022, doi: 10.1108/SR-09-2021-0315.

[11] C. Berri *et al.*, "Predicting the quality of meat: Myth or reality?" *Foods*, vol. 8, no. 10, p. 436, Sep. 2019, doi: 10.3390/foods8100436.

[12] J.-L. Damez and S. Clerjon, "Quantifying and predicting meat and meat products quality attributes using electromagnetic waves: An overview," *Meat Sci.*, vol. 95, no. 4, pp. 879–896, Dec. 2013, doi: 10.1016/j.meatsci.2013.04.037.

[13] D. L. Phelps *et al.*, "The surgical intelligent knife distinguishes normal, borderline and malignant gynaecological tissues using rapid evaporative ionisation mass spectrometry (REIMS)," *Brit. J. Cancer*, vol. 118, no. 10, pp. 1349–1358, May 2018, doi: 10.1038/s41416-018-0048-3.

[14] K. Shahzada, A. Yurkewich, R. Xu, and R. Patel, "Sensorization of a surgical robotic instrument for force sensing," *Proc. SPIE*, vol. 9702, Mar. 2016, Art. no. 97020U.

[15] A. Mason, D. Romanov, L. E. Cordova-Lopez, and O. Korostynska, "Smart knife for robotic meat cutting," in *Proc. IEEE Sensors*, Oct./Nov. 2021, pp. 1–4, doi: 10.1109/SENSORS47087.2021.9639793.

[16] A. Mason *et al.*, "Theoretical basis and application for measuring pork loin drip loss using microwave spectroscopy," *Sensors*, vol. 16, no. 2, p. 182, Feb. 2016, doi: 10.3390/s16020182.

[17] B. Egelandsdal *et al.*, "Detectability of the degree of freeze damage in meat depends on analytic-tool selection," *Meat Sci.*, vol. 152, pp. 8–19, Jun. 2019, doi: 10.1016/j.meatsci.2019.02.002.

[18] S. G. Bjarnadottir, K. Lunde, O. Alvseike, A. Mason, and A. I. Al-Shamma'a, "Assessing quality parameters in dry-cured ham using microwave spectroscopy," *Meat Sci.*, vol. 108, pp. 109–114, Oct. 2015, doi: 10.1016/j.meatsci.2015.06.004.

[19] A. Mason, M. Muradov, B. Abdullah, A. Al-Shamma'a, and O. Alvseike, "Rapid non-destructive prediction of water activity in dry-cured meat," *Proceedings*, vol. 2, no. 13, p. 1003, 2018. [Online]. Available: https://www.mdpi.com/2504-3900/2/13/1003.

[20] V. S. Nisa, S. Rajesh, K. P. Murali, V. Priyadarsini, S. N. Potty, and R. Ratheesh, "Preparation, characterization and dielectric properties of temperature stable $SrTiO_3$/PEEK composites for microwave substrate applications," *Compos. Sci. Technol.*, vol. 68, no. 1, pp. 106–112, Jan. 2008, doi: 10.1016/j.compscitech.2007.05.024.

[21] A. Listrat *et al.*, "How muscle structure and composition influence meat and flesh quality," *Sci. World J.*, vol. 2016, Oct. 2016, Art. no. 3182746, doi: 10.1155/2016/3182746.

[22] *NanoRFE*. Accessed: Apr. 7, 2022. [Online]. Available: https://nanorfe.com/nanovna-v2.html

[23] *Node-RED*. Accessed: Apr. 7, 2022. [Online]. Available: https://nodered.org

[24] A. Mason, O. Korostynska, and L. E. Cordova-Lopez, "Sensorised knife-blade cutting system," U.K. Patent 2 108 679.8, Jun. 17, 2021.

A. Mason received the B.Sc. (Hons.) degree in computer and multimedia systems from the University of Liverpool, Liverpool, U.K., in 2005, and the Ph.D. degree in wireless sensor networks and their industrial applications from Liverpool John Moores University (LJMU), Liverpool, in 2008.

From 2008 to 2017, he performed research related to sensor technology and led a Research Team at LJMU related to this topic. He moved to Norway in 2017 to take a position as a Project Engineer for Animalia AS, Oslo, Norway, where he develops sensor and automation technology for the meat sector. In 2018, he also joined the Norwegian University of Life Sciences (NMBU), Ås, Norway, where he became a Research Professor in 2020 after establishing a team working on food automation. He has approximately 250 peer-reviewed publications, which include several patents. He currently coordinates the Horizon 2020 Project RoBUTCHER.

D. Romanov received the B.Sc. degree in system engineering and the M.Sc. degree in automation and computer-integrated technologies from Odesa National Polytechnic University (ONPU), Odesa, Ukraine, in 2017 and 2018, respectively. He is currently pursuing the Ph.D. degree with the Norwegian University of Life Sciences (NMBU), Ås, Norway.

His research interests include application of robotics for automation in the red meat industry, development of human–robot collaborative approaches to the meat processing, and intelligent sensing in robotics.

L. E. Cordova-Lopez received the B.Sc. (Hons.) degree from the University of Liverpool, Liverpool, U.K., in 2005, and the Ph.D. degree in the field of microwave plasmas for the remediation of internal combustion exhaust gases from Liverpool John Moores University, Liverpool, in 2009.

From 2010 to 2019, he has worked as a full-time Researcher and a Lecturer with the Faculty of the Built Environment, Liverpool John Moores University, researching in the areas of building and environmental services, LabVIEW, low carbon economy, environmental legislation systems and management, and in sensors for the health industry. Since 2020, he has been a full-time Researcher of the H2020 Project RoBUTCHER at REALTEK, Norwegian University of Life Sciences (NMBU), Norway.

O. Korostynska received the B.Eng. and M.Sc. degrees from the National Technical University of Ukraine (KPI), Kyiv, Ukraine, in 1998 and 2000, respectively, and the Ph.D. degree in electronics and computer engineering from the University of Limerick, Limerick, Ireland, in 2003.

She is a Professor of Biomedical Engineering with Oslo Metropolitan University (OsloMet), Oslo, Norway, and an Associate Professor with the Norwegian University of Life Sciences (NMBU), Ås, Norway. Her research interests include various sensors and their applications, specifically semiconductor, polymer, and electromagnetic wave sensors, including for real-time water quality monitoring and biomedical applications. She is part of the RoBUTCHER Project Team, developing a smart knife for automated cutting in meat industry. She has coauthored two books, 15 book chapters, five U.K. patents, and more than 300 scientific papers in peer-reviewed journals and conference proceedings.